Amino Acids (2008) 35: 389–396
DOI 10.1007/s00726-007-0604-2
Printed in The Netherlands

Amino Acids

Computational studies of the binding modes of A_{2A} adenosine receptor antagonists

Y. Ye[1], **J. Wei**[1], **X. Dai**[2], and **Q. Gao**[2]

[1] School of Pharmaceutical Science and Technology, Tianjin University, Tianjin, China
[2] Chemistry Department, XenoPort Inc., Santa Clara, CA, U.S.A.

Received August 10, 2007
Accepted September 12, 2007
Published online November 5, 2007;

Summary. A molecular docking study was performed on several structurally diverse A_{2A} AR antagonists, including xanthines, and non-xanthine type antagonists to investigate their binding modes with A_{2A} adenosine receptor (AR), one of the four subtypes of AR, which is currently of great interest as a target for therapeutic intervention, in particular for Parkinson's disease. The high-affinity binding site was found to be a hydrophobic pocket with the involvement of hydrogen bonding interactions as well as $\pi-\pi$ stacking interactions with the ligands. The detailed binding modes for both xanthine and non-xanthine type A_{2A} antagonists were compared and the essential features were extracted and converted to database searchable queries for virtual screening study of novel A_{2A} AR antagonists. Findings from this study are helpful for elucidating the binding pattern of A_{2A} AR antagonists and for the design of novel active ligands.

Keywords: Adenosine receptors – A_{2A} AR antagonists – Binding mode – Docking – Pharmacophore – Virtual screening

Introduction

Adenosine receptors (AR) belong to the super-family of seven transmembrane domain G protein-coupled receptors. Four subtypes (A_1, A_{2A}, A_{2B}, and A_3) of receptors have been cloned and characterized (Fredholm et al., 2001). ARs are found in a wide variety of tissues and preside over panoply of biological effects. It is known that A_{2A} and A_{2B} receptors can activate adenylate cyclase while A_1 and A_3 receptors cause the reverse effects (Hourani et al., 2001). As a result, the ligands of these receptors are desirable for pharmacological and medicinal studies, in particular for the treatment of serious disorders such as hypoxia, asthma, and Parkinson's disease.

Stimulation of A_{2A} AR has recently been found to reduce the binding affinity of dopamine D_2 receptors (Ongini et al., 1997; Richardson et al., 1997) and participate in the inhibition of tumor necrosis factor-α, IL-6, and IL-8 (Elenkov et al., 2000). In addition, A_{2A} AR is abnormally increased in cells expressing mutant huntingtin (Varani et al., 2001). Therefore, A_{2A} AR antagonists have become a great interest for therapeutic intervention, in particular for the treatment of Parkinson's disease.

Over the last decades, many A_{2A} AR antagonists including xanthine and non-xanthine derivatives have been proposed. As a major series of all A_{2A} AR antagonists, xanthine A_{2A} antagonists suffer from low selectivity and poor pharmacophysiological properties (Nonaka et al., 1993; Müller et al., 1997, 1998; Sauer et al., 2000). The xanthine type adenosine antagonist theophylline and its closely related analog caffeine have been used clinically as antiasthmatic agents based on their weak adenosine antagonistic activity (Feokistov and Biaggioni, 1998), but their usage is associated with unpleasant side effects, such as insomnia and diuresis (Vassalo and Lipsky, 1998). To overcome the above-mentioned shortcomings, non-xanthine type heterocyclic A_{2A} antagonists are later developed, as demonstrated recently in the two main classes of bicyclic and tricyclic non-xanthine derivatives (Barbara et al., 2003; Vu et al., 2004a, b; Matasi et al., 2005). The encouraging results especially for the increased selectivity from non-xanthine type analogs further stimulate interest of scientist to develop more structurally diverse antagonists as useful therapeutic agents.

The seven AR transmembrane domains are connected by three extracellular and three intracellular hydrophilic loops (Bockaert and Pin, 1999). Given that these macromolecules could not be easily crystallized to have their

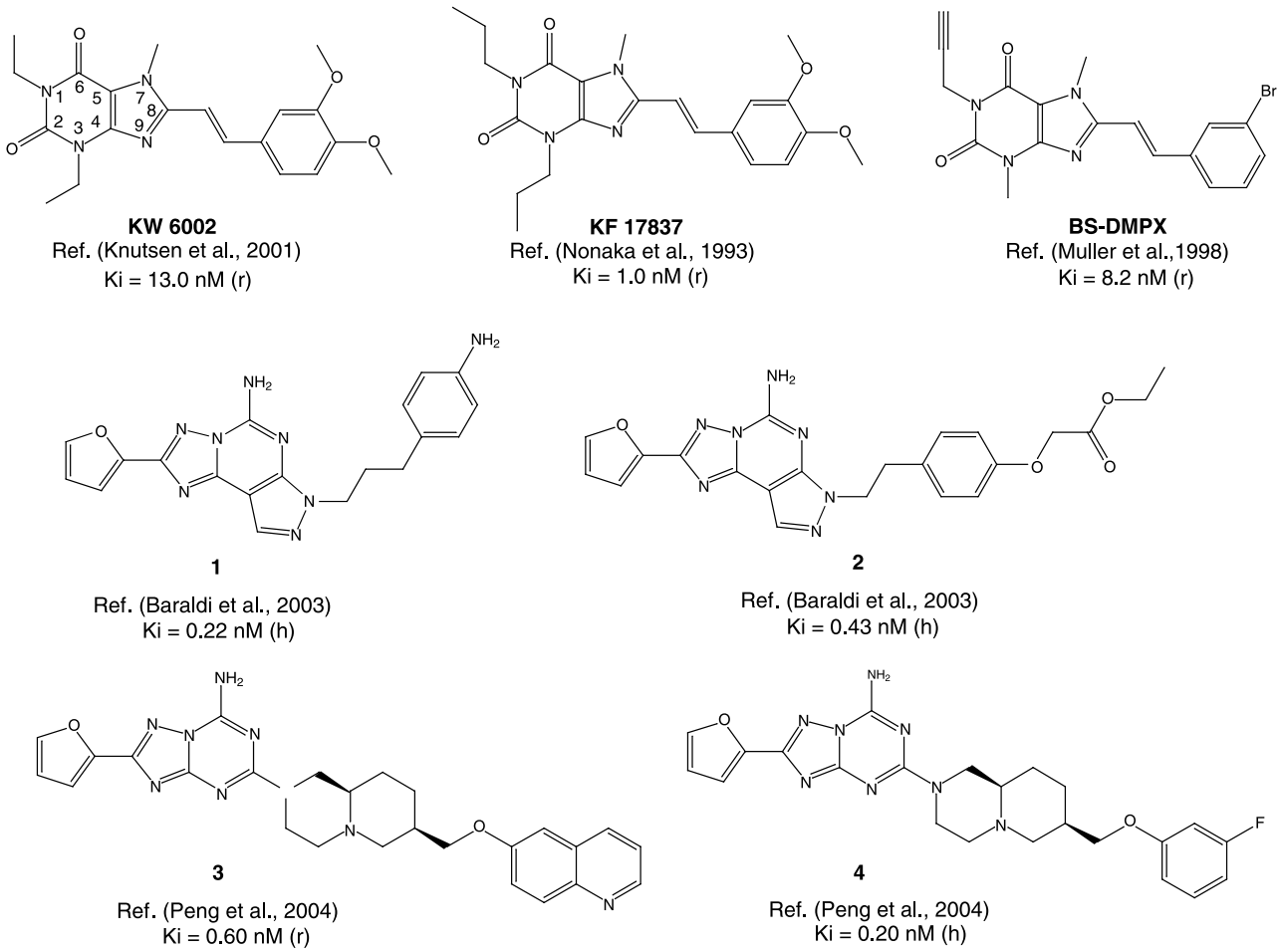

Fig. 1. Compounds selected for docking study and SAR analysis. (*r* rat; *h* human)

structures elucidated via X-ray crystallography, 3D structural models of adenosine receptors including A_{2A} AR have been constructed using homology modeling method based on the structure of bovine rhodopsin whose data of X-ray diffraction were published lately (Ivanov et al., 2002, 2003, 2005; Stefano et al., 2005). Our recent study on 3D pharmacophore models of selective A_{2A} and A_{2B} AR antagonists demonstrated that the ligand-based approach is very useful for analyzing the ligand-receptor interactions (Wei et al., 2007). However, no systematic receptor-based docking study has been reported in this field especially using non-xanthine type AR antagonists.

The aim of the present work is to use molecular modeling to characterize the binding modes of different types of A_{2A} AR antagonists, in particular to differentiate between the xanthine type antagonists and non-xanthine derivatives. The docking process in this study can be used as a computational tool to design novel selective A_{2A} AR antagonists. The results from the binding mode analysis and the pharmacophoric observation may also be useful

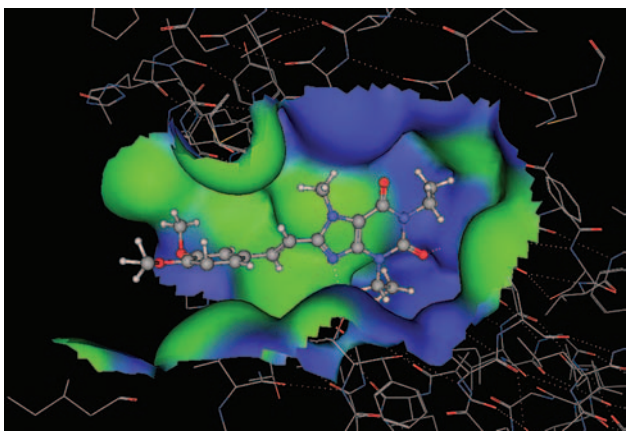

Fig. 2. Theoretical models of the A_{2A} binding site complexed with compound **KW6002**. The molecular surface is color-coded by hydrophobicity properties. The green is for hydrophobic, blue for hydrophilic. The constituents of the pocket are defined by those residues within a distance of 6 Å from the ligands. For a better illustration of the binding modes, residues at one side of the pocket are hidden (for an interpretation of the reference to colour in this figure, the reader is referred to the online version of this paper under www.springerlink.com)

in rational drug discovery and can be integrated with molecular docking process for virtual screening of A_{2A} AR antagonists.

Materials and methods

The molecular docking technique can provide many useful clues and insights for drug designs (Chou et al., 2003, 2006; Chou, 2004e, 2006; Du et al., 2004, 2005a, 2007a, b; Sirois et al., 2004; Wei et al., 2005, 2006a, b, 2007; Zhang et al., 2006; Gui et al., 2007; Wang et al., 2007a, c, d). In this study, seven structurally diverse A_{2A} AR antagonists (Fig. 1), including highly selective non-xanthine type A_{2A} AR antagonists were chosen as the training set for docking study. All A_{2A} AR antagonists were modeled within the ViewCompound workbench using Catalyst 4.11 and optimized with the Amber99 force field using Chimera. Each compound was docked using DOCK5.4 to the active binding site of the A_{2A} adenosine receptor whose structural data had been recently released from RCSB Protein Data Bank (PDB entry 1MMH). All graphic manipulations and visualizations were performed by means of the Chimera program, while ligand docking was performed using DOCK 5.4. Generation of database searchable pharmacophores were executed using Catalyst 4.11 which installed on aIBM6223I2C work station equipped with aIntel Xeon processor (3.0 GHz) and 1GB of RAM running the RedHat WS3.0 operating system.

Results and discussion

According to Chou et al. (1999), the binding pocket was defined by those residues that have at least one heavy atom (i.e., an atom other than hydrogen) with a distance ≤ 5 Å from a heavy atom of the ligand. Such a definition has been widely and successfully used for investigating

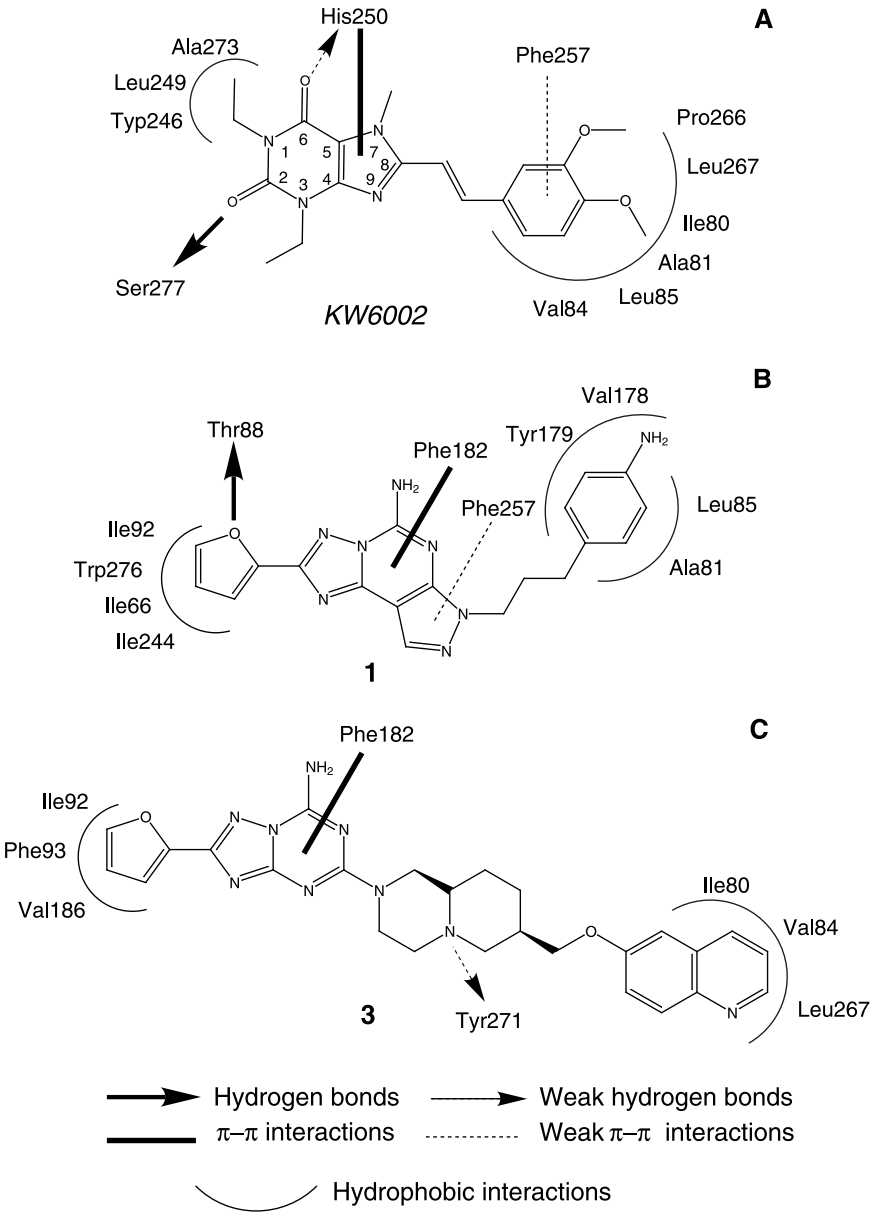

Fig. 3. Binding mode of the A_{2A} antagonists. (**A**) Binding mode of **KW6002**, (**B**) Binding mode of compound **1**. (**C**) Binding mode of compound **3**

various protein-ligand interactions (Chou et al., 2000; Chou, 2004a, b, c, d; Sirois et al., 2004; Chou, 2005a, b; Du et al., 2005a, b; Wei et al., 2006a, b, 2007; Zhang et al., 2006; Gao et al., 2007; Li et al., 2007; Wang et al., 2007a, b). In this work, with the docking program, we identified that the active binding pocket of the A_{2A} AR antagonists was surrounded by five transmembrane helices (TM2, TM3, TM5, TM6, and TM7). This finding is consistent with the results from site-directed mutagenesis studies (Kim et al., 1995).

In order to determine the residues involved in the stable binding interactions between the antagonists and A_{2A} AR, we first performed molecular docking study using three most potent xanthine type antagonists: **KW6002** ((*E*)-1,3-diethyl-8-(3,4-dimethoxystyryl)-7-methyl-xanthine, Ki = 13 nM), **KF17837** ((*E*)-1,3-dipropyl-8-(3,4-dimethoxystyryl)-7-methyl-xanthine, Ki = 1 nM), and **BS-DMPX** ((*E*)-3,7-dimethyl-1-propargyl-8-(3-bromostyryl)-xanthine, Ki = 8.2 nM) (Baraldi et al., 2002). According to the results from the antagonistic activity studies, all (*E*)-isomers of 8-styryl substituted xanthine type antagonists are more potent than (*Z*)-isomers. We focused our docking analysis on the Energy Scores of only (*E*)-configurations on the styryl side chains. The outcome of the docking analysis indicates that all three xanthine type antagonists have similar binding mode patterns.

In Fig. 2, the interaction pattern obtained for **KW6002**, a clinical candidate for Parkinson's disease (Knutsen and Weiss, 2001), suggests that the side chain phenyl ring of the molecule points to the cell surface while the xanthine moiety occupies the bottom of the binding pocket. As the binding mode illustrated in Fig. 3A, the hydroxyl group of Ser277 forms a hydrogen bond with the carbonyl oxygen at the 2-position of the xanthine moiety. In addition, another weak hydrogen bonding interaction between the NH group of His250 and the oxygen at the 6-position may also contribute to the affinity of the ligand to the receptor. A hydrophobic pocket, delimited by Typ246, Leu249, and Ala273, interacts with the ethyl substituent at the 1-position of the xanthine moiety. Amino acids Ile92, Ser91, and His278 (not shown in Fig. 3) along with the above-mentioned residues (Typ246, Leu249, and Ala273) constitute the bottom of this binding pocket, which accommodates the whole xanthine moiety of the ligand. Additionally, His250 interacts with the imidazole ring of the xanthine structure with a π–π interaction. This result is in good agreement with mutagenetic studies in which the change of His250 to Ala leads to the loss of antagonism whereas the replacement of His250 with Phe or Tyr has no effect on the antagonist's binding affinity (Kim et al., 1995). The phenyl ring of this highly potent antagonist and its two methoxy groups are located at the entrance of the binding pocket, which is largely occupied by hydrophobic residues such as Pro266, Leu267, Ile80, Ala81, Val84, and Leu85. A weak π–π stacking interaction between this phenyl group and Phe257 is also predicted.

The binding mode of **KF17837** is virtually the same as that of **KW6002**. The xanthine moieties of these two ligands reside in a similar position, whereas the aromatic group on the side chain falls in the hydrophobic pocket interacting with the corresponding residues. However, Tyr179 is involved in the ligand binding via a strong π–π interaction with the phenyl moiety of **KF17837**.

The data obtained for **BS-DMPX**, a highly selective A_{2A} xanthine type antagonist, suggest that the arrangement of the phenyl group of this ligand is similar to that of **KF17837**, and the single meta-substituent is involved in the hydrophobic interaction with Val84 on the pocket surface. The phenyl rings of Phe257 and Tyr179 are within a strong π–π interaction distance from the 8-styryl substituent. Unlike the other two ligands, the xanthine moiety of this ligand flips over oriented in the binding pocket. According to the docking result of this molecule, only one hydrogen bonding interaction is observed between the carbonyl oxygen of the 6-position of the xanthine moiety with Thr88, while no significant interaction is found for the other carbonyl group. The propargyl group on the 1-position of the xanthine core occupies

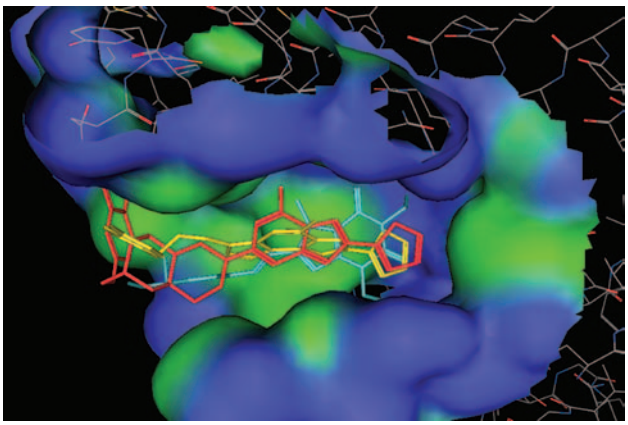

Fig. 4. Molecular surface of the active pocket of A_{2A} adenosine receptor. **KW6002** (*cyan*), compound **1** (*yellow*) and compound **3** (*red*) are docked in the binding pocket. The molecular surface is color-coded by hydrophobicity properties. The green is for hydrophobic, blue for hydrophilic. The constituents of the pocket are defined by those residues within a distance of 6 Å from the ligands. For a better illustration of the binding modes, residues at one side of the pocket are hidden (for an interpretation of the reference to colour in this figure, the reader is referred to the online version of this paper under www.springerlink.com)

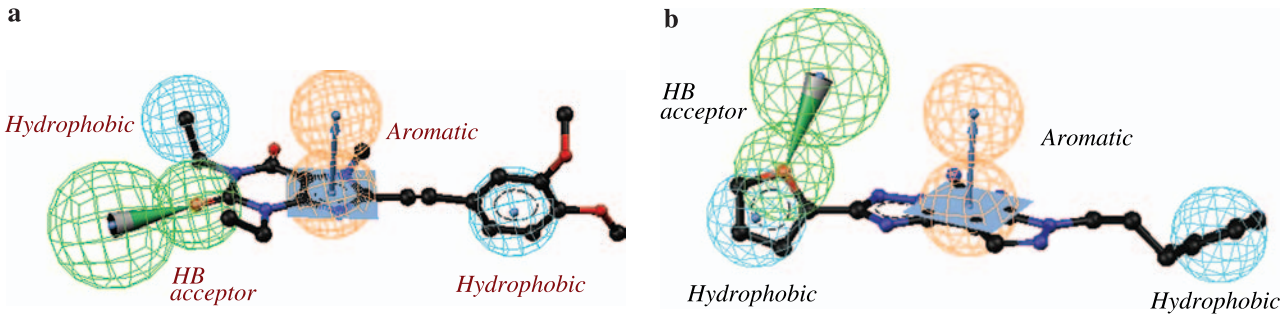

Fig. 5. Extracted pharmacophore models based on binding mode from docking analysis. (**A**) A representative of four featured pharmacophore model from xanthine type A_{2A} antagonist. (**B**) A representative of four featured pharmacophore model from non-xanthine type A_{2A} antagonist. Pharmacophore features are color-coded: green represents hydrogen bond acceptor; orange represents ring aromatic; light blue represents hydrophobic (for an interpretation of the reference to colour in this figure, the reader is referred to the online version of this paper under www.springerlink.com)

the hydrophobic site surrounded by Ile92 and His278, which is opposite to the site taken by the other two compounds due to the flip over of the xanthine plane.

As for the docking study with non-xanthine type A_{2A} AR antagonists, we first evaluated compound **1**, which has a strong binding affinity (Ki = 0.22 nM) with high selectivity ($Ki_{A1}/Ki_{A2A} = 9818$, $Ki_{A2B}/Ki_{A2A} > 45455$, and $Ki_{A3}/Ki_{A2A} > 45455$) (Barbara et al., 2003). The binding model from the docking analysis suggests that the small furan ring is embedded deeply down at the bottom of the binding pocket delimited by Ile244, Ile66, Trp276, and Ile92 (Fig. 3B and Fig. 4) whereas the xanthine type antagonists are prohibited from a deep interposition to this extent due to their structural bulkiness of xanthine group. A hydrogen bond between the oxygen on the furan moiety and the hydroxyl group of Thr88 is predicted to be an important interaction within this pocket. The pyrazole ring of the tricyclic structure is predicted to be involved in a π–π interaction with Phe257, whereas another π–π stacking interaction between Phe182 and the central pyrimidine ring is also regarded to be important for the molecular binding. This result is in line with the finding from mutagenetic studies (Kim et al., 1995). The aniline moiety on the side chain points to the extracellular environment and interacts with the hydrophobic surface shaped by Tyr179, Val178, Leu85, and Ala81 at the entrance of the binding pocket.

The binding pattern for compound **2** shows that the arrangement of the tricyclic moiety of this ligand is similar to that for compound **1**. An additional hydrogen bonding interaction between the N atom at the 3-position of the tricyclic structure and Thr88 is also involved in the ligand binding. However, due to the significant difference between the side chains of these two compounds, the phenyl ring of compound **2** lies in a different hydrophobic surface surrounded by Val84 and Leu85, while the ethyl group of its ester moiety interacts with the hydrophobic residues of Ile80 and Ala81.

As illustrated in Fig. 3C, non-xanthine antagonist compound **3** presents a similar binding mode on the bicyclic moiety to that of the tricyclic derivatives **1** and **2**. However, the furan ring lies in a new pocket delimited by Ile92, Phe93, and Val186 and thus loses the hydrogen bonding with Thr88. Only a weak hydrogen bond interaction was observed between the bridge N atom of the piperazine structure and Tyr271. The quinoline moiety at the end of the side chain forms a strong interaction with a hydrophobic surface shaped by Ile80, Val84, and Leu267.

The only difference between compounds **4** and **3** is at the side chain aromatic ring moiety. Therefore, a very similar binding mode was observed for compound **4** with the increased magnitude of the π–π interaction between the triazine ring and Phe182.

By combining the docking results from above discussed xanthine and non-xanthine type A_{2A} AR antagonists, we were able to extract some binding mode features, which

Table 1. Binding energies of ligands derived from the docking procedure (kcal/mol)

Ligands[a]	E_{total}[b]	E_{vdw}[c]	E_{ele}[d]
KW6002	−41.562	−40.728	−0.834
KF17837	−47.895	−47.226	−0.669
BS-DMPX	−40.800	−40.919	0.119
1	−39.045	−39.654	0.609
2	−42.409	−42.454	0.045
3	−43.244	−43.549	0.305
4	−42.384	−43.552	1.168

[a] Energy results for 8-styryl substituted xanthine type antagonists (**KW6002**, **KF17837**, and **BS-DMPX**) are from (*E*)-configurations of the styryl side chain. [b] Total binding energies for each antagonists in kcal/mol. [c] Van der Waals contribution to the binding free energies for each antagonists. [d] Electrostatic energy as calculated by the AMBER99 force field of DOCK 5.4.

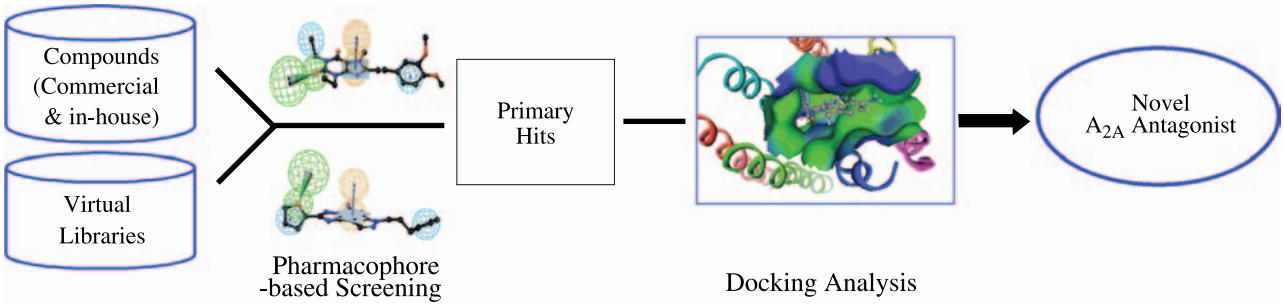

Fig. 6. Proposed virtual screening approach for novel A_{2A} antagonist

could be essential for different ligands as potential A_{2A} AR antagonists and convert them into database searchable pharmacophore models. Figure 5 illustrates two examples of such pharmacophore models. Both xanthine (Fig. 5A) and non-xanthine antagonists (Fig. 5B) share similar π–π interaction between the antagonists and the corresponding aromatic residues. In addition, there are at least two hydrophobic interaction zones at both ends of the molecules. A hydrogen bonding interaction from each type of the antagonists may also play an important role in the A_{2A}-specific binding and antagonist recognition.

Finally, in order to integrate our docking study into a routine drug design and screening process, providing rapid evaluation of binding affinities for a virtual library of potential antagonists, we calculated the solvent-free lowest binding energy for each antagonist-receptor complex using the energy scoring function implemented in the DOCK program (Table 1). The total interaction energies, consisting of van der Waals and electrostatic components, for the three xanthine type antagonists (**KW6002**, **KF17837**, and **BS-DMPX**) were substantially on the same level reflecting the similar Ki value for these antagonists. The binding energy scores for the non-xanthine type A_{2A} AR antagonists (**1**, **2**, **3**, and **4**), ranging from −39 to −42 kcal/mol, also indicate the similar interaction level as all ligands have strong receptor binding affinity (Ki = 0.2 to 0.6 nM).

With the structure-based docking analysis and the database searchable pharmacophores retrieved through the binding mode study, we are considering a combination strategy to increase the accuracy as well as the efficiency of virtual screening process for the novel A_{2A} AR antagonists (Fig. 6). The pharmacophore-based screening step acts as a filtering system for both commercial/in-house compound libraries and virtually designed target focused libraries. The pharmacophores derived from the xanthine type antagonists can first remove the existing xanthine or caffeine derivatives and then pick up structurally novel compounds as potential A_{2A} antagonist, whereas the non-xanthine type antagonist derived pharmacophore models may directly function as probes to identify new substrates as potential antagonistic ligands. The primary hits from this pharmacophore-based screening analysis will be further evaluated by the docking study to efficiently identify the true positives. Both pharmacophore-based screening step and structure-based docking analysis are integrated with scoring functions (in Catalyst, best fit value can be calculated as fit score) that make this combination approach a convenient and practical tool applicable to other virtual screening projects.

Conclusions

Based on the results of this molecular docking study, we propose a general binding mode of the selective A_{2A} AR antagonists and define the residues involved in receptor-ligand recognition. For xanthine type A_{2A} antagonists, the models demonstrate that Ser277 could be essential to the hydrogen bonding formation with the carbonyl group at the 2-position of the ligands, while His250, and Phe257 could be involved in the stable ligand binding because of their π–π interactions with the antagonists. Moreover, the hydrophobic interaction domains located at both the entrance and the bottom of the binding pocket are supposed to make important contributions to the binding affinity of all A_{2A} AR antagonists.

As for the class of non-xanthine ligands, two adjacent hydrophobic sites (one delimited by residues, Ile92, Trp276, Ile66, and Ile244; the other by residues Ile92, Phe93, and Val186) accommodate the furan moiety along with a hydrophobic pocket which interacts with the side chains to support the basic binding of the ligands. Weak hydrogen bonding interactions at the furan oxygen or piperazine nitrogen may contribute to the binding affinity, and the π–π interactions between residues: Phe182 and Phe257 with the heterocyclic moiety of the ligands pro-

vide additional driving force for stable binding of the non-xanthine type A_{2A} AR antagonists.

Based on the extracted interaction modes, a series of database searchable pharmacophore models have been created to represent different combinations of important binding interactions for A_{2A} antagonists. These pharmacophore models are useful to identify potential new A_{2A} antagonists in the proposed pharmacophore-based virtual screening approach. The molecular docking analysis from this study can be used either as a structure-based drug design tool, or it can be integrated with the pharmacophore-based virtual screening approach in order to enhance the accuracy of the virtual screening and improve the enrichment of the true positives.

Acknowledgements

This work was supported by the Tianjin Municipal Science and Technology Commission (#043186011) of the Ministry of Science and Technology of the People's Republic of China. We would like to thank Songmei Li, and Wei Wang of NEOTRIDENT as well as Dr. Brian Sung at Accelrys Inc. for their dedicated support.

References

Baraldi PG, Cacciari B, Romagnoli R, Spalluto G, Monopoli A, Ongini E, Varani K, Borea PA (2002) 7-Substituted 5-amino-2-(2-furyl)pyrazolo[4,3-e]-1,2,4-triazolo[1,5-c]pyrimidines as A2A adenosine receptor antagonists: a study on the importance of modifications at the side chain on the activity and solubility. J Med Chem 45: 115–126

Barbara C, Giorgia P, Giampiero S (2003) Medicinal chemistry of A2A adenosine receptor antagonists. Curr Top Med Chem 3: 403–411

Bockaert J, Pin JP (1999) Molecular tinkering of G protein-coupled receptors: an evolutionary success. EMBO J 18: 1723–1729

Chou KC (2004a) Insights from modelling the 3D structure of the extracellular domain of alpha7 nicotinic acetylcholine receptor. Biochem Biophys Res Commun 319: 433–438

Chou KC (2004b) Insights from modelling the tertiary structure of BACE2. J Proteome Res 3: 1069–1072

Chou KC (2004c) Modelling extracellular domains of GABA-A receptors: subtypes 1, 2, 3, and 5. Biochem Biophys Res Commun 316: 636–642

Chou KC (2004d) Molecular therapeutic target for type-2 diabetes. J Proteome Res 3: 1284–1288

Chou KC (2004e) Review: structural bioinformatics and its impact to biomedical science. Curr Med Chem 11: 2105–2134

Chou KC (2005a) Coupling interaction between thromboxane A2 receptor and alpha-13 subunit of guanine nucleotide-binding protein. J Proteome Res 4: 1681–1686

Chou KC (2005b) Modeling the tertiary structure of human cathepsin-E. Biochem Biophys Res Commun 331: 56–60

Chou KC (2006) Structural bioinformatics and its impact to biomedical science and drug discovery. In: Atta-ur-Rahman, Reitz AB (eds) Frontiers in medicinal chemistry, vol. 3. Bentham Science Publishers, The Netherlands, pp 455–502

Chou KC, Tomasselli AG, Heinrikson RL (2000) Prediction of the tertiary structure of a caspase-9/inhibitor complex. FEBS Lett 470: 249–256

Chou KC, Watenpaugh KD, Heinrikson RL (1999) A model of the complex between cyclin-dependent kinase 5(Cdk5) and the activation domain of neuronal Cdk5 activator. Biochem Biophys Res Commun 259: 420–428

Chou KC, Wei DQ, Du QS, Sirois S, Zhong WZ (2006) Review: progress in computational approach to drug development against SARS. Curr Med Chem 13: 3263–3270

Chou KC, Wei DQ, Zhong WZ (2003) Binding mechanism of coronavirus main proteinase with ligands and its implication to drug design against SARS (Erratum: ibid., 2003, vol. 310, 675). Biochem Biophys Res Commun 308: 148–151

Du QS, Wang S, Wei DQ, Sirois S, Chou KC (2005a) Molecular modelling and chemical modification for finding peptide inhibitor against SARS CoV Mpro. Anal Biochem 337: 262–270

Du QS, Wang SQ, Jiang ZQ, Gao WN, Li YD, Wei DQ, Chou KC (2005b) Application of bioinformatics in search for cleavable peptides of SARS-CoV Mpro and chemical modification of octapeptides. Med Chem 1: 209–213

Du QS, Wang SQ, Wei DQ, Zhu Y, Guo H, Sirois S, Chou KC (2004) Polyprotein cleavage mechanism of SARS CoV Mpro and chemical modification of octapeptide. Peptides 25: 1857–1864

Du QS, Sun H, Chou KC (2007a) Inhibitor design for SARS coronavirus main protease based on "distorted key theory". Med Chem 3: 1–6

Du QS, Wang SQ, Chou KC (2007b) Analogue inhibitors by modifying oseltamivir based on the crystal neuraminidase structure for treating drug-resistant H5N1 virus. Biochem Biophys Res Commun; doi: 10.1016/j.bbrc.2007.08.025

Elenkov IJ, Chrousos GP, Wilder RL (2000) Neuroendocrine regulation of IL-2 and TNF-alpha/IL-10 balance, clinical implications. Ann NY Acad Sci 917: 94–105

Feokistov I, Biaggioni I (1998) Pharmalogical characterization of adenosine A2B receptors. Biochem Pharmacol 55: 627–633

Fredholm BB, IJzerman AP, Jacobson KA, Klotz KN, Linden J (2001) International union of pharmacology, XXV. Nomenclature and classification of adenosine receptors. Pharmacol Rev 53: 527–552

Gao WN, Wei DQ, Li Y, Gao H, Xu WR, Li AX, Chou KC (2007) Agaritine and its derivatives are potential inhibitors against HIV proteases. Med Chem 3: 221–226

Gui XL, Li L, Wei DQ, Zhu YS, Chou KC (2007) Cleavage mechanism of the H5N1 hemagglutinin by trypsin and furin. Amino Acids (in press)

Hourani SM, Boon K, Fooks HM, Prentice DJ (2001) Role of cyclic nucleotides in vasodilations of the rat thoracic aorta induced by adenosine analogues. Br J Pharmacol 133: 833–840

Ivanov AA, Baskin II, Palyulin VA, Piccagli L, Baraldi PG, Zefirov NS (2005) Molecular modeling and molecular dynamics simulation of the human A2B adenosine receptor. The study of the possible binding modes of the A2B receptor antagonists. J Med Chem 48: 6813–6820

Ivanov AA, Baskin II, Palyulin VA, Zefirov NS (2002) Molecular modeling the human A1 adenosine receptor and study of the mechanisms of its selective ligand binding. Dokl Biochem Biophys 386: 271–274

Ivanov AA, Baskin II, Palyulin VA, Zefirov NS (2003) Molecular modeling of the human A2A adenosine receptor. Dokl Biochem Biophys 389: 94–97

Kim J, Wess J, van Rhee AM, Schöneberg T, Jacobson KA (1995) Site-directed mutagenesis identifies residues involved into ligand recognition in the human A2A adenosine receptor. J Biol Chem 270: 13987–13997

Knutsen LJ, Weiss SM (2001) kw-6002 (Kyowa Hakko Kogyo). Curr Opin Invest Drugs 2: 668–673

Li L, Wei DQ, Wang JF, Chou KC (2007) Computational studies of the binding mechanism of calmodulin with chrysin. Biochem Biophys Res Commun 358: 1102–1107

Matasi JJ, Caldwell JP, Hao J, Neustadt B, Arik L, Foster CJ, Lachowicz J, Tulshian DB (2005) The discovery and synthesis of novel adenosine receptor (A2A) antagonists. Bioorg Med Chem Lett 15: 1333–1336

Müller CE, Geis U, Hipp J, Schobert U, Frobenius W, Pawlowski M, Suzuki F, Sandoval-Ramírez J (1997) Synthesis and structure-activity relationship of 3,7-dimethyl-1-propargylxanthine derivatives, A2A-selective adenosine receptor antagonists. J Med Chem 40: 4396–4405

Müller CE, Sandoval-Ramírez J, Schobert U, Geis U, Frobenius W, Klotz K (1998) N,8-(Sulfostyryl)xanthines: water-soluble A2A-selective adenosine receptor antagonists. Bioorg Med Chem 6: 707–719

Nonaka Y, Shimada J, Nonaka H, Koike N, Aoki N, Kobayashi H, Kase H, Yamaguchi K, Suzuki F (1993) Photoisomerization of a potent and selective adenosine A2 antagonist, (E)-1,3-dipropyl-8-(3,4-dimethoxystyryl)-7-methylxanthine. J Med Chem 36: 3731–3733

Ongini E, Adami M, Ferri C, Bertorelli R (1997) Adenosine A2A receptors and neuroprotection. Ann NY Acad Sci 825: 30–48

Richardson PJ, Kase H, Jenner PG (1997) Adenosine A2A receptor antagonists as new agents for the treatment of Parkinson's disease. Trends Pharmacol Sci 18: 338–344

Sauer R, Maurinsh J, Reith U, Fülle F, Klotz KN, Müller CE (2000) Water-soluble phosphate prodrugs of 1-propargyl-8-styrylxanthine derivatives, A2A-selective adenosine receptor antagonists. J Med Chem 43: 440–448

Sirois S, Wei DQ, Du QS, Chou KC (2004) Virtual screening for SARS-CoV protease based on KZ7088 pharmacophore points. J Chem Inf Comput Sci 44: 1111–1122

Stefano M, Giampiero S, Kenneth AJ (2005) Techniques: recent developments in computer-aided engineering of GPCR ligands using the human adenosine A3 receptor as an example. Trends Pharmacol Sci 25: 44–51

Vassalo R, Lipsky JJ (1998) Theophylline: recent advances in the understanding of its mode of action and uses in clinical practice. Mayo Clin Proc 73: 346–354

Varani K, Rigamonti D, Sipione S, Camurri A, Borea PA, Cattabeni F, Abbracchio MP, Cattaneo E (2001) Aberrant amplification of A2A receptor signaling in striatal cells expressing mutant huntingtin. FASEB 15: 1245–1247

Vu CB, Peng B, Kumaravel G, Smits G, Jin X, Phadke D, Engber T, Huang C, Reilly J, Tam S, Grant D, Hetu G, Chen L, Zhang J, Petter RC (2004a) Piperazine derivatives of [1,2,4]triazolo-[1,5-a][1,3,5] triazine as potent and selective adenosine A2A receptor antagonists. J Med Chem 47: 4291–4299

Vu CB, Shields P, Peng B, Kumaravel G, Jin X, Phadke D, Wang J, Engber T, Ayyub E, Petter RC (2004b) Triamino derivatives of triazolotriazine and triazolopyrimidine as adenosine A2a receptor antagonists. Bioorg Med Chem Lett 14: 4835–4838

Wang JF, Wei DQ, Li L, Zheng SY, Li YX, Chou KC (2007a) 3D Structure modeling of cytochrome P450 2C19 and its implication for personalized drug design. Biochem Biophys Res Commun (Corrigendum: ibid, 2007, vol. 357, 330) 355: 513–519

Wang JF, Wei DQ, Lin Y, Wang YH, Du HL, Li YX, Chou KC (2007b) Insights from modeling the 3D structure of NAD(P)H-dependent D-xylose reductase of Pichia stipitis and its binding interactions with NAD and NADP. Biochem Biophys Res Commun 359: 323–329

Wang SQ, Du QS, Chou KC (2007c) Study of drug resistance of chicken influenza A virus (H5N1) from homology-modeled 3D structures of neuraminidases. Biochem Biophys Res Commun 354: 634–640

Wang SQ, Du QS, Zhao K, Li AX, Wei DQ, Chou KC (2007d) Virtual screening for finding natural inhibitor against cathepsin-L for SARS therapy. Amino Acids 33: 129–135

Wei DQ, Sirois S, Du QS, Arias HR, Chou KC (2005) Theoretical studies of Alzheimer's disease drug candidate [(2,4-dimethoxy) benzylidene]-anabaseine dihydrochloride (GTS-21) and its derivatives. Biochem Biophys Res Commun 338: 1059–1064

Wei DQ, Du QS, Sun H, Chou KC (2006a) Insights from modeling the 3D structure of H5N1 influenza virus neuraminidase and its binding interactions with ligands. Biochem Biophys Res Commun 344: 1048–1055

Wei DQ, Zhang R, Du QS, Gao WN, Li Y, Gao H, Wang SQ, Zhang X, Li AX, Sirois S, Chou KC (2006b) Anti-SARS drug screening by molecular docking. Amino Acids 31: 73–80

Wei H, Zhang R, Wang C, Zheng H, Chou KC, Wei DQ (2007) Molecular insights of SAH enzyme catalysis and their implication for inhibitor design. J Theor Biol 244: 692–702

Wei J, Wang S, Gao S, Dai X, Gao Q (2007) 3D-Pharmacophore models for selective A_{2A} and A_{2B} adenosine receptor antagonists. J Chem Inf Model 47(2): 613–625

Zhang R, Wei DQ, Du QS, Chou KC (2006) Molecular modeling studies of peptide drug candidates against SARS. Med Chem 2: 309–314

Authors' address: Qingzhi Gao, Chemistry Department, XenoPort Inc., 3410 Central Expressway, Santa Clara, CA 95051, U.S.A.,
Fax: (408) 616-7210, E-mail: qingzhi@gmail.com